Designing a more nonlinearly stable laminar flow via boundary manipulation

By S. M. E. RABIN[1], C. P. CAULFIELD[2,1]† AND R. R. KERSWELL[3]

[1]Department of Applied Mathematics & Theoretical Physics, Centre for Mathematical Sciences, University of Cambridge, Wilberforce Road, Cambridge CB3 0WA, UK

[2]BP Institute, University of Cambridge, Madingley Rise, Madingley Road Cambridge CB3 0EZ, UK

[3]School of Mathematics, University of Bristol, BS8 1TW Bristol, UK

(Received 7 November 2013; revised ?; accepted ?. - To be entered by editorial office)

We show how a fully nonlinear variational method can be used to design a more nonlinearly stable laminar shear flow by quantifying the effect of manipulating the boundary conditions of the flow. Using the example of plane Couette flow, we demonstrate that by forcing the boundaries to undergo spanwise oscillations in a certain way, it is possible to increase the critical disturbance energy for the onset of turbulence by 41%. If this is sufficient to ensure laminar flow (i.e. ambient noise does not exceed this increased threshold), nearly four times less energy is consumed than in the turbulent flow which exists in the absence of imposed spanwise oscillations.

1. Introduction

There is a considerable ongoing effort directed at manipulating turbulent flows to either reduce their drag or relaminarise them completely (see for example the recent reviews of Kasagi *et al.* (2009) and Quadrio (2011)). The latter relaminarisation challenge can be restated as the problem of delaying the onset of turbulence by some controlled adjustment of the laminar flow. So far, theoretical work has concentrated on probing the sensitivity of the linearised dynamics around the laminar state to disturbances in order to design suitable controls. This approach has had some success in mitigating turbulence transition using both open-loop and feedback-based approaches (Kim & Bewley (2007)). For example, Högberg *et al.* (2003) used direct numerical simulation to demonstrate that linear feedback control strategies can expand the laminar state's basin of attraction significantly for a range of flow Reynolds numbers. Also, in a channel flow subject to streamwise travelling waves (induced by zero-net-mass-flux wall blowing and suction), Moarref & Jovanović (2010) used a perturbation analysis in the wave amplitude of the linearised Navier-Stokes equations to 'design' travelling waves which significantly reduce the flow's sensitivity. This suggested a viable control of turbulence transition which was confirmed by fully nonlinear direct numerical simulation of the flow (Lieu *et al.* (2010)).

However, delaying the onset of turbulence in shear flows is a fully nonlinear problem. Transition is triggered by finite-amplitude background disturbances and immediately results in a temporally and spatially complex final state (see for example Schmid & Henningson (2001); Mullin & Kerswell (2005); Manneville (2008)) rather than progressing

† Email address for correspondence: c.p.caulfield@bpi.cam.ac.uk

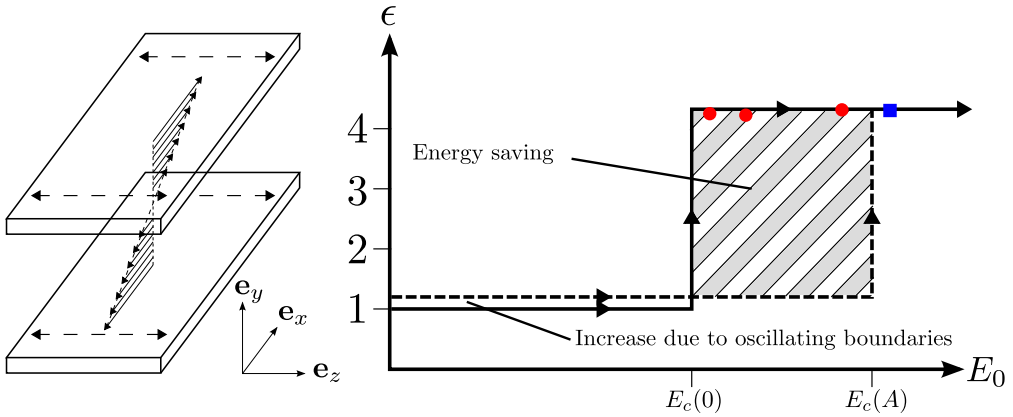

FIGURE 1. a) Schematic flow geometry showing coordinate system, laminar flow profile (solid lines) and spanwise boundary oscillation (dashed lines). b) Schematic to illustrate how delaying transition can save energy. The symbols indicate actual average dissipation rate data (relative to the laminar unoscillated PCF value) from numerical simulations: red dots are for unoscillated PCF and the blue square is for spanwise-oscillated PCF (note the turbulent dissipation rate for oscillated PCF is very similar to that for unoscillated PCF).

through a series of bifurcations triggered by an initial linear instability of the laminar state. Therefore, as discussed by Bewley (2001), there is a clear need for a fully nonlinear approach to investigate the sensitivity of the laminar state to finite amplitude disturbances. This means understanding how the basin of attraction of the laminar state changes when the flow is intentionally modified (for example by moving the boundaries in a new way exemplified by Kawahara (2005)). In particular, if the point of minimal 'amplitude' (typically defined in terms of disturbance kinetic energy) on the basin boundary for the laminar state can be quantifiably shown to move away (i.e. towards higher values of initial disturbance energy) from the laminar state with a control, then the effectiveness of the control is demonstrated.

Recently, just such a new theoretical method has emerged which allows the *nonlinear* stability of a flow to be probed (see Pringle & Kerswell (2010); Cherubini *et al.* (2010); Monokrousos *et al.* (2011); Pringle *et al.* (2012); Rabin *et al.* (2012); Cherubini & De Palma (2013); Duguet *et al.* (2013) for applications to the Navier-Stokes equations, and Juniper (2011) for an application to an idealised model of thermo-acoustics). This is a variational method which seeks to maximise a functional (such as the disturbance kinetic energy or the time- and space-integrated total dissipation) over all possible initial disturbances of a given initial magnitude (with respect to some norm) which evolve subject to the governing Navier-Stokes equations to a large but finite time horizon. The result of this optimisation is then tracked as the initial disturbance norm is gradually increased until a sudden jump is generically seen. This jump corresponds to the first instance of the optimisation method encountering an initial disturbance lying outside the basin of attraction under scrutiny. The increased value of the functional signals by design the new (possibly turbulent) end-state of the subsequent evolution. Crucially, this method constructively delivers the spatial structure of the disturbance of lowest energy - christened the *minimal seed* in Pringle *et al.* (2012) - as well as the threshold value of this chosen norm (typically the kinetic energy).

The central aim of this paper is to demonstrate the potential of this relatively new fully nonlinear method for developing strategies to control flows. The specific setting used here to illustrate our method is the simplest example of a shear flow - plane Couette flow

(PCF) - in which a layer of fluid of kinematic viscosity ν is sheared between two infinite parallel plates at $y = \pm h$ which move with velocities $\pm U\mathbf{e_x}$. The simple shear basic state, as shown in figure 1a, is linearly stable for all Reynolds numbers $Re := Uh/\nu$ (Romanov (1973)) yet transition to turbulence is observed experimentally at Re as low as 325 (Bottin & Chate (1998)). This transition is undesirable as the energy dissipation rate significantly increases in the turbulent state. To enhance the nonlinear stability of this low-dissipation basic state, we investigate the effect of superimposing spanwise oscillations of the boundaries such that

$$\mathbf{u}(x, \pm 1, z, t) = \pm \mathbf{e_x} + A \sin(\omega t + 2\pi\phi)\mathbf{e_z} \tag{1.1}$$

where h and h/U are the units of distance and time, A is the amplitude, ω the frequency and ϕ the phase of the oscillation. This choice is motivated by the large body of work which has demonstrated (experimentally and through direct numerical simulations) that such boundary motion can reduce *turbulent* drag by up to 40% (see Jung *et al.* (1992); Laadhari *et al.* (1994); Baron & Quadrio (1996); Quadrio (2011), and also Moarref & Jovanović (2012); Duque-Daza *et al.* (2012) for recent theoretical work).

The aim in those studies was to ameliorate the consequences of turbulence *after* it has been triggered whereas here the focus is to *delay* the onset of turbulence (see figure 1b), i.e. to 'prevent' rather than 'cure' turbulence. In more formal dynamical systems parlance, the previous work has investigated how spanwise boundary oscillations affect the turbulent attractor, whereas here we now investigate how spanwise boundary oscillations affect the basin of attraction of the underlying basic state. Interestingly, this modification of the basin of attraction leads to a qualitative change in the structure of the minimal seed from that which has recently been identified for unoscillated PCF (Monokrousos *et al.* (2011); Rabin *et al.* (2012); Duguet *et al.* (2013)) due to the nontrivial modification of the base flow in the immediate vicinity of the driving plates. In section 2, we describe our nonlinear variational method and show how spanwise boundary oscillation increases the critical initial perturbation energy of the minimal seed which can trigger turbulence. In section 3 we discuss the change in the structure and properties of the minimal seed due to spanwise boundary oscillation, showing the role played by the phase ϕ of the oscillation in the time-evolution of minimal seeds towards turbulence. Finally, section 4 offers some concluding remarks.

2. Variational Method

When the boundaries are oscillated, the basic fluid response to the enforced boundary motion (1.1) is $\mathbf{u} = \mathbf{U} := y\mathbf{e_x} + W(y, t; A)\mathbf{e_z}$ and

$$W = A[f(y)\sin(\omega t + 2\pi\phi) + g(y)\cos(\omega t + 2\pi\phi)], \tag{2.1}$$

with

$$f = \cosh y^+ \cos y^- + \cosh y^- \cos y^+)/\Lambda, \tag{2.2}$$

$$g = -(\sinh y^+ \sin y^- + \sinh y^- \sin y^+)/\Lambda, \tag{2.3}$$

where

$$\theta = \sqrt{\omega Re/2},\ y^\pm = \theta(1 \pm y) \text{ and } \Lambda = \cos 2\theta + \cosh 2\theta. \tag{2.4}$$

The difference of the fluid response from the basic state, $\hat{\mathbf{u}} = \mathbf{u} - \mathbf{U}$ (hereafter the disturbance velocity) evolves under the Navier-Stokes equations

$$\frac{\partial}{\partial t}\hat{\mathbf{u}} + \mathbf{U}.\boldsymbol{\nabla}\hat{\mathbf{u}} + \hat{\mathbf{u}}.\boldsymbol{\nabla}\mathbf{U} + \hat{\mathbf{u}}.\boldsymbol{\nabla}\hat{\mathbf{u}} + \boldsymbol{\nabla}\hat{p} = \frac{1}{Re}\nabla^2\hat{\mathbf{u}}, \tag{2.5}$$

with incompressibility and the natural boundary conditions imposed:

$$\boldsymbol{\nabla}\cdot\hat{\mathbf{u}}=0,\ \hat{\mathbf{u}}(x,\pm1,z,t)=\mathbf{0}. \tag{2.6}$$

If $\hat{E}(t):=\langle\frac{1}{2}\hat{\mathbf{u}}(\mathbf{x},t)^2\rangle$ is the disturbance kinetic energy (where $\langle\ \rangle$ is a volume average), then nonlinear stability can be quantified by the minimum initial disturbance kinetic energy for which the long time state is *not* the basic state,

$$E_c(A):=\min_{\hat{\mathbf{u}}(\mathbf{x},0):\hat{\mathbf{u}}(\mathbf{x},t\to\infty)\neq\mathbf{0}}\hat{E}(0)=\langle\frac{1}{2}\hat{\mathbf{u}}(\mathbf{x},0)^2\rangle. \tag{2.7}$$

Here that means turbulence is triggered (the dependence of E_c on Re and ω is suppressed for clarity). Recently, we found (see Rabin *et al.* (2012) for more details of our method and the results) that $E_c(0)=2.232\times10^{-6}$ for $Re=1000$ using a fully nonlinear variational method (Pringle *et al.* (2012)) in a computational box 4.08π-periodic in x and 1.05π-periodic in z with a time horizon $T\approx300$. Our nonlinear variational method determines the spatial structure of the incompressible initial velocity perturbation with given initial perturbation kinetic energy which maximises perturbation kinetic energy at a certain target time, by a four-step algorithm, effectively a nonlinear generalization of the 'direct-adjoint' looping algorithm as described in Schmid (2007). In the first step, an initial condition guess of the disturbance 'forward' flow velocity $\hat{\mathbf{u}}(0)$ with initial disturbance energy $\hat{E}_0$ is integrated 'forwards' as a solution of the nonlinear Navier-Stokes equations (2.5) to a target time T to yield $\hat{\mathbf{u}}(T)$. In the second step, this final flow velocity is rescaled to yield a terminal state of the 'adjoint' velocity field $\mathbf{v}(T)=\hat{\mathbf{u}}(T)/E_0$. This adjoint velocity field is then integrated 'backwards' in time from $t=T$ to $t=0$ as a solution of the nonlinear adjoint Navier-Stokes equations

$$\frac{\partial}{\partial t}\mathbf{v}+(\mathbf{U}+\hat{\mathbf{u}}).\boldsymbol{\nabla}\mathbf{v}-(\boldsymbol{\nabla}\otimes[\hat{\mathbf{u}}+\mathbf{U}]).\mathbf{v}+\boldsymbol{\nabla}q=\frac{1}{Re}\nabla^2\mathbf{v}, \tag{2.8}$$

where, using the Einstein summation convention, $[(\boldsymbol{\nabla}\otimes\mathbf{u}).\mathbf{v}]_i=v_j\partial u_j/\partial x_i$, and q is an adjoint 'pressure' imposing incompressibility. If $\mathbf{v}(0)$ does **not** have exactly the same spatial structure as $\hat{\mathbf{u}}(0)$, then the fourth step of the algorithm is to use some appropriate search algorithm (such as steepest descent) to update the initial guess $\hat{\mathbf{u}}(0)$, so that when passing again around the direct-adjoint loop, the adjoint disturbance velocity eventually satisfies $\mathbf{v}(0)\approx c\hat{\mathbf{u}}(0)$ to within some tolerance for some constant c.

This iterative algorithm is a strategy to solve the Euler-Lagrange equations of a variational problem to maximise the disturbance energy gain $\hat{E}(T)/\hat{E}(0)$ at a target time T subject to various constraints imposed by Lagrange multipliers: the constant c imposing the initial disturbance energy $\hat{E}(0)$; the pressures $\hat{p}$ and q imposing the incompressibility of $\hat{\mathbf{u}}$ and $\mathbf{v}$ respectively; and the adjoint velocity field $\mathbf{v}(\mathbf{x},t)$ imposing the requirement that $\hat{\mathbf{u}}$ satisfies the full nonlinear three-dimensional 'forward' Navier-Stokes equations (2.5). Setting to zero the variations of the Lagrangian including the disturbance energy gain subject to these constraints with respect to $\hat{\mathbf{u}}$ yields the requirement that $\mathbf{v}$ satisfies the nonlinear three-dimensional 'adjoint' Navier-Stokes equations (2.8). As in Rabin *et al.* (2012), we use a modified version of the Diablo CFD solver (Taylor (2008)), which is spectral in x and z and finite-difference in y, to solve these forward and adjoint equations, using resolutions up to $128\times1536\times32$ to ensure adequate convergence. Such high resolution in the cross-stream $y-$direction seemed to help convergence when the initial energy $\hat{E}(0)$ of perturbation was close to E_c, otherwise a lower resolution of 256 was perfectly adequate. Direct numerical simulation confirms that the modified base flow remains linearly stable for $A<1$. If it is not, $E_c(A)=0$ as defined in (2.7) and our optimisation algorithm cannot be applied.

3. Results

To explore if E_c can be increased with A, we fix $Re = 1000$, adopt the same geometry as in Rabin *et al.* (2012), i.e. 4.08π-periodic in x and 1.05π-periodic in z, and again choose the disturbance energy gain $\hat{E}(T)/\hat{E}(0)$ as the key functional to be optimised, using a fixed long target time horizon of $T = 300$. In unoscillated flow at the same Reynolds number, this target time is sufficiently large to identify whether the flow will undergo the transition to turbulence or not for the accuracy in $\hat{E}(0)$ sought (Rabin *et al.* (2012)). For example, reducing the energy of the minimal seed in the unoscillated situation by 1.4% clearly leads to relaminarisation by $t = T$ (see figure 7 of Rabin *et al.* (2012)). The oscillation frequency is chosen as $\omega = 0.01$ so that the boundary oscillation modifies the interior flow significantly (the nondimensional Stokes boundary layer width $1/\sqrt{\omega Re}$ is ≈ 0.3) yet is large enough so that the induced flow is still significantly time-varying over the timescale T for disturbances to reach turbulence. For this size of ω and the accuracy to which we work (3 significant figures in $\hat{E}(0)$), whether an initial disturbance decays or triggers transition is still clearly discernible by $T = 300$.

The presence of the phase ϕ in the wall oscillations means the variational calculations (which study the fate of disturbances added at $t = 0$) must be run for each $\phi \in [0, \frac{1}{2})$ to deliver a threshold energy $E_c^\phi(A, \phi)$ which depends on ϕ. Note that $E_c(-A) = E_c(A)$ so the results for $\phi \in [\frac{1}{2}, 1)$ repeat those for $[0, \frac{1}{2})$. The overall threshold energy for transition for disturbances which are introduced at any time (but then are assumed to evolve in isolation) is then

$$E_c(A) = \min_{0 \leqslant \phi < \frac{1}{2}} E_c^\phi(A, \phi). \tag{3.1}$$

Figure 2a shows how $E_c(A)/E_c(0)$ varies with A. Unsurprisingly, large values of A ($>$ 0.4) lead to destabilization at reduced initial energies compared to the unoscillated flow. However, oscillations with $A < 0.4$ actually increase $E_c(A)$ above $E_c(0)$, and for the 'best choice' of $A = 0.35$, $E_c(A) \in (3.01, 3.02) \times 10^{-6}$ so $E_c(A)/E_c(0) = 1.35 \pm 0.01$ which is a significant improvement of nonlinear stability. An exploratory set of computations varying ω actually gave our overall best stabilization result for $A = 0.35$ and $\omega = 0.01333$. For these parameters, we found $E_c(A) \in (3.15, 3.16) \times 10^{-6}$, corresponding to $E_c(A)/E_c(0) = 1.41$, as plotted on 2a with a red square. The substantial variation of $E_c^\phi(A, \phi)$ with ϕ (see figure 2b) as well as A suggests that not only the magnitude of the background oscillation, but also its timing relative to the growth of nonlinear perturbations are significant in delaying transition to turbulence. For the choice of parameters $A = 0.35$, $\omega = 0.01$, a phase of $\phi = 0.485$ yielded $E_c(A)$. Of interest is the apparently anomalously high value of $E_c^\phi(0.35, 0.31)$, and we discuss the reasons for this below.

To understand the apparent stabilizing effect of the boundary oscillation, we examine the spatial and temporal behaviour of the *minimal seed*, labelled S_0 and of initial disturbance energy $E_c(0)$, which is the first disturbance as $\hat{E}(0)$ increases to trigger transition in unoscillated PCF ($A = 0$). This disturbance S_0 is localised away from the walls to minimise its kinetic energy yet retains sufficient nonlinearity to trigger transition (Rabin *et al.* (2012), top left plot in figure 3). Rescaling this disturbance from initial energy $E_c(0) \approx 2.232 \times 10^{-6}$ to 3.01×10^{-6}, i.e. just below $E_c(0.35)$ leads to turbulence at $T \approx 100$ (and $A = 0$), well before the time horizon of $T \approx 300$ in the variational calculations, at which turbulence would only just be reached for $\hat{E}(0) = E_c(0)^+$. Cross-sections of the evolving flow (left panels of figure 3) show that the disturbance quickly expands under shearing to produce large scale streaks (regions of faster and slower flowing fluid in the streamwise direction) which fill the channel and then break down to small scales predominantly at the wall (see Pringle *et al.* (2012) and Duguet *et al.* (2013) for more

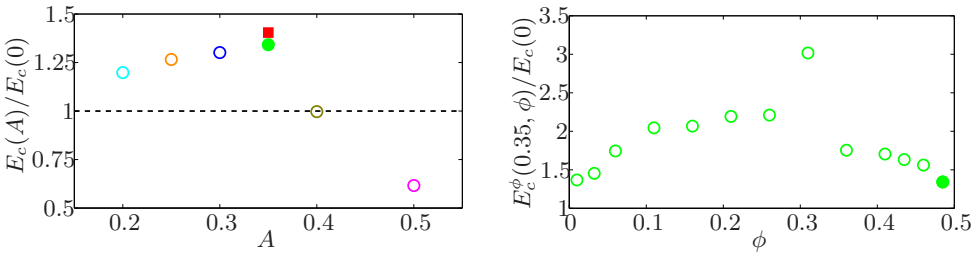

FIGURE 2. a) Estimated values (plotted with filled circles) or upper bounds given by $E_c^\phi(A,\phi)/E_c(0)$ for some ϕ (hollow circles) of $E_c(A)/E_c(0)$ for various amplitudes A of oscillation at $\omega = 0.01$. Our overall best stabilization result of $E_c(A) \in (3.15, 3.16) \times 10^{-6}$ at $A = 0.35$ and $\omega = 0.01333$ corresponding to $E_c(A)/E_c(0) = 1.41$ is shown as a red square. b) $E_c^\phi(0.35,\phi)/E_c(0)$ for various values of phase ϕ and $\omega = 0.01$. The minimum value $E_c(0.35) \simeq 1.35$ occurs for $\phi = 0.485$ and is plotted with a solid symbol.

details of the sequential hierarchy of the growth mechanisms of such minimal seeds). Interestingly, if the boundary oscillation is switched on with $A = 0.35$ and $\omega = 0.01$, the evolution is very different with the flow relaminarising even if S_0 is further rescaled to have initial energy slightly above $E_c(0.35)$ at 3.02×10^{-6} (not shown).

The structure and evolution of the associated minimal seed, labelled S_A for the oscillated flow ($A = 0.35$ and $\omega = 0.01$) and rescaled down slightly to the same energy $\hat{E}(0) = 3.01 \times 10^{-6} \lesssim E_c(0.35)$, changes significantly. The right panels of figure 3 show the same initial mid-channel localisation but the subsequent globalisation of the disturbance with time is noticeably different. Now the preferred (lowest starting energy) route to transition is one in which the large scale streaks produced clearly avoid the spanwise shear set up near the oscillating walls, typically located within 0.5 of the walls at ± 1. The clear implication is that the spanwise shear set up by the oscillating wall inhibits the small-scale breakdown of the streaks due to 'bending' near the walls as discussed in detail by Cherubini *et al.* (2011) and Duguet *et al.* (2013). In fact, streaks have trouble forming near the wall in the first place as they get smeared out by the spanwise shear (note this effect is absent for steady spanwise motion of the walls which simply advects the streaks as a whole). So E_c is not only increased by spanwise oscillation, but importantly the form of the minimal seed too is changed qualitatively. To reiterate this, the flow evolutions of the two situations are shown in figure 3. They are clearly different, with the unoscillated PCF (left panels) remaining turbulent, while the oscillated PCF eventually relaminarises, as the initial energy $\hat{E}(0)$ has been scaled to a value just below the critical value $E_c(0.35)$ for transition.

To understand better how the spanwise shear affects the flow we examine the volume-averaged spanwise shear rate squared, $H := \langle (dW/dy)^2 \rangle$, whose dependence on ϕ (or equivalently on time, since $\omega = 0.01$, $\phi \in [0, 1]$ corresponds to $t \in [0, 200\pi]$) is shown in figure 4a. The black dots mark the initial values of ϕ of the various minimal seeds whose scaled initial energy is plotted against ϕ in figure 2b. The time evolutions of the disturbance energies of these various minimal seeds are plotted in figure 4b, and they demonstrate that, irrespective of ϕ, all of the minimal seeds require a similar amount of time to 'unpack' and approach the spatially-global 'edge state' (relative attractor on the laminar-turbulent boundary), in a manner discussed in Rabin *et al.* (2012). Subsequent to reaching the energy plateau where the edge state exists it appears that the initial value of ϕ heavily influences how long the flow remains close to the edge state before transitioning to turbulence. On both plots in figure 4 we have marked $\phi = 0.15$ and 0.3 (also due to periodicity 0.65 and 0.8), as between these values of ϕ the spanwise shear,

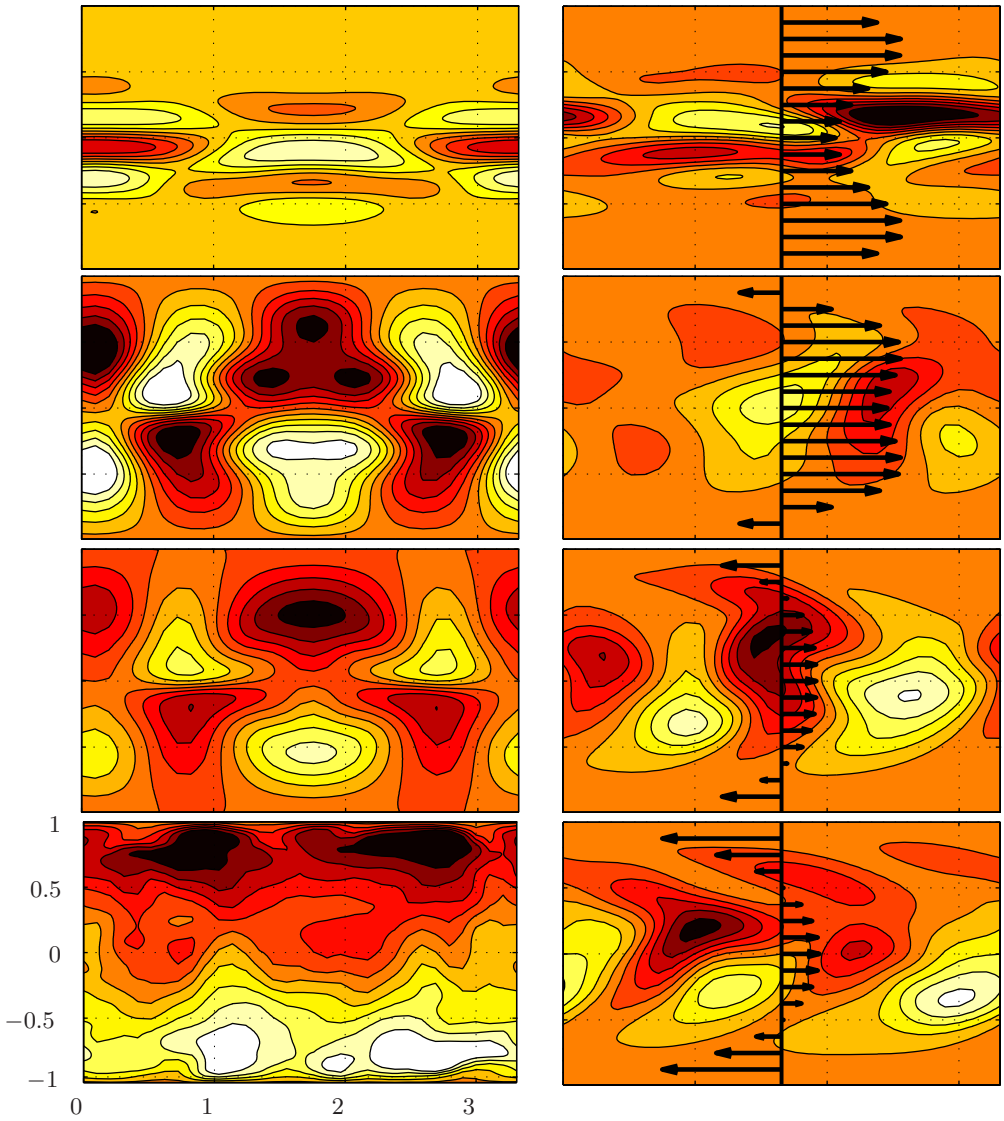

FIGURE 3. Contours of the streamwise disturbance velocity (streaks) $\hat{\mathbf{u}}.\mathbf{e_x}$ at $t = 0$, 48, 88 and 128 for the evolving minimal seeds S_0 (left for $A = 0$) and S_A (right for $A = 0.35$), both rescaled to $E_c(0) < \hat{E}(0) = 3.01 \times 10^{-6} \lesssim E_c(0.35)$. Red/dark indicate negative values and white/light indicates positive values with 10 contours drawn across the following ranges: top left down to bottom left $[-0.001, 0.0006]$, $[-0.1, 0.1]$, $[-0.4, 0.5]$, $[-0.6, 0.6]$; top right to bottom right $[-0.0025, 0.0015]$, $[-0.2, 0.2]$, $[-0.2, 0.2]$, $[-0.2, 0.2]$. The black arrows on the right plot indicate $W(y,t)$ to highlight the changing spanwise shear near the walls ($W = 0$ on the left for unoscillated PCF and $\phi = 0.485$ on the right).

H attains its maximum value and also because between these values of ϕ it appears that no flow transitions from the edge state to turbulence. This appears to support our previous conclusion that the spanwise shear disrupts the bending and destabilization of the streamwise streaks which is the process that triggers the breakdown of the edge state.

Armed with this we can begin to understand why $E_c^\phi(0.35, \phi)/E_c(0)$ varies so significantly with ϕ and specifically why $E_c^\phi(0.35, 0.485)/E_c(0)$ is minimal and why

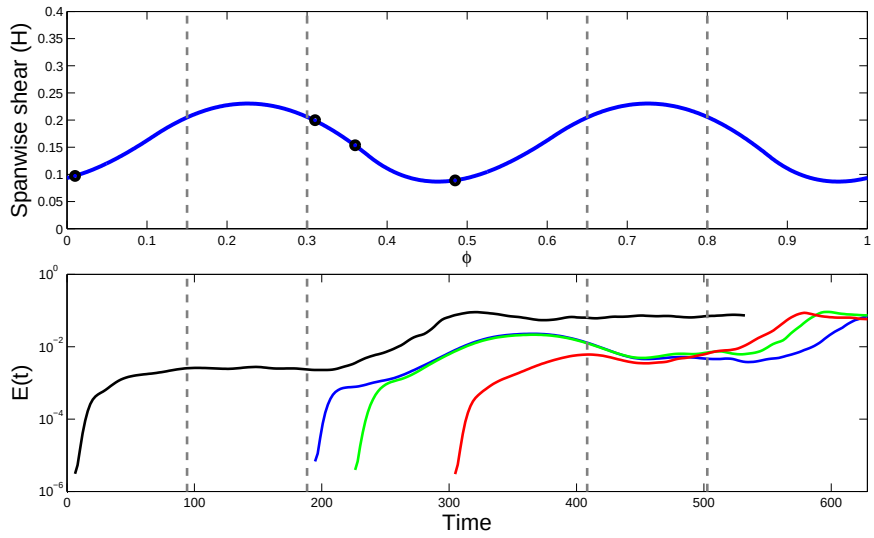

FIGURE 4. a) Time variation of $H = \langle (dW/dy)^2 \rangle$ against ϕ. Black dots indicate values of ϕ for which the time evolution of disturbance energy $\hat{E}(t)$ is presented below. The time interval shown as $\phi \in [0, 1]$ corresponds to $t \in [0, 200\pi]$. b) Time evolution of $\hat{E}(t)$ against t over the same time interval as panel a) for ϕ =0.01 (black line), 0.31 (blue line), 0.36 (green line), and 0.485 (red line). The vertical dashed grey lines indicate the time intervals, associated with the integrated spanwise shear where no flow appears to undergo transition from near the edge state to turbulence. Note the variation of the initial $E_c^{\phi}(0.35, \phi)$ of the different minimal seeds, in particular the relatively large initial value for the $\phi = 0.31$ case and the relatively small initial value for the $\phi = 0.485$ case. Each solution goes through three characteristic stages: an 'unpacking' and growth from an initially localised perturbation to the characteristic edge state energy level with $\hat{E} \sim O(10^{-3})$; a certain period of closeness to the edge state; and then an ultimate transition to turbulence with further elevation of energy to $\hat{E} \sim O(10^{-1})$.

$E_c^{\phi}(0.35, 0.31)/E_c(0)$ is so much higher than the surrounding values. It appears that for $\phi = 0.485$ (plotted with a red line) the duration of the initial 'unpacking' phase is such that by the time the seed has 'unpacked' and approached the edge state the quantity H has passed its maximum and is already decreasing, and so the shear rate is sufficiently low to allow the flow to transition. Therefore because the flow remains close to the edge state for a relatively short period of time the initial perturbation can have a lower energy, as it is able to bypass the longer periods of time that other seeds must spend close to the edge state. Effectively, it has arrived at the edge state just in time to 'catch' the extra streak bending which triggers streak break down and hence transition. Although not quite so well-timed, the behaviour for $\phi = 0.01$ (plotted with a black line) is quite similar, in that the flow remains close to the edge state for a relatively short time before undergoing the transition to turbulence (recall the dynamics is periodic across $\phi \in [0, \frac{1}{2}]$).

Conversely, for $\phi = 0.31$ (plotted with a blue line) it appears that the initial unpacking phase ensures that the minimal seed arrives just too late at the edge state, and so it has 'missed' its opportunity to undergo transition during the first low H time interval. Therefore, although it can grow in amplitude during this low H time interval, it must 'wait' close to the edge state for an extended period of time until it is able to 'catch' the next opportunity for extra streak bending to trigger transition. Thus, in order that the flow remains close to the edge for an extended period, this particular minimal seed

requires a considerably larger initial energy than other seeds. For a neighbouring larger value of the phase $\phi = 0.36$ (plotted with a green line) the initial energy amplitude is somewhat smaller as the amplification during the initial 'unpacking' phase is stronger, but the subsequent evolution close in the vicinity of the edge state is very similar.

Imposing the spanwise oscillation at a fixed constant amplitude (an active, open-loop control) consumes energy through driving the spanwise base flow W against viscous dissipation, and it is only worthwhile if there is an overall energy saving. The dissipation rate D_B of the full base flow $\mathbf{U} = y\mathbf{e_x} + W\mathbf{e_z}$ is defined as

$$D_B = \frac{1}{Re}\overline{\langle|\boldsymbol{\nabla}\mathbf{U}|^2\rangle} = \frac{1}{Re}\left[1 + \frac{A^2\theta}{2}\left(\frac{\sinh(2\theta) - \sin(2\theta)}{\cosh(2\theta) + \cos(2\theta)}\right)\right] \tag{3.2}$$

and takes the value $D_B \approx 1.14/Re = 1.14D_{B0}$ for the case $A = 0.35$ and $Re = 1000$ where the overline signifies averaging over one period of spanwise oscillation, and $D_{B0} = 1/Re$ is the dissipation rate of the unoscillated basic laminar PCF $y\mathbf{e_x}$. In comparison, the turbulent dissipation rate is approximately $4.3D_{B0}$, as shown in figure 1b. Thus, if the system is operating in an environment where the ambient noise has (kinetic energy) amplitude between $E_c(0)$ and $E_c(0.35)$, there should be a clear power saving of $\approx 3.1D$ in maintaining the shear across the plates, as represented by the shaded region in figure 1b. The use of the word 'should' is deliberate since the computations described here have considered only the 'simplest' fully nonlinear problem of disturbing the Navier-Stokes equations with *one* finite-amplitude disturbance at *one* point in time. Studying a multiply or continuously disturbed system is obviously the next step towards reality.

It is also worth noting that our stabilization result is not simply a renormalisation effect. Augmenting the base flow $y\mathbf{e_x}$ by a spanwise oscillation $W(y,t)\mathbf{e_z}$ suggests that Re should be renormalised to a higher value based on the combined average speed of the walls. This would (generically) be expected to lower the threshold for transition (e.g. Peixinho & Mullin (2007)). Instead, we have demonstrated an increase in the threshold brought about by a qualitatively different, and more energetic base flow. One could also argue that the threshold energy needs to be rescaled with the new underlying base energy which includes the spanwise flow. Once again averaging over one period of spanwise oscillation, the kinetic energy E_B in the oscillating base flow can be shown to be

$$E_B = \frac{1}{2}\overline{\langle|\mathbf{U}|^2\rangle} = \frac{1}{6}\left[1 + \frac{3A^2}{4\theta}\left(\frac{\sinh(2\theta) + \sin(2\theta)}{\cosh(2\theta) + \cos(2\theta)}\right)\right] \approx \frac{1.04}{6} = 1.04E_{B0}, \tag{3.3}$$

for the case $A = 0.35$ and $Re = 1000$, where the unoscillated PCF flow has background kinetic energy $E_{B0} = 1/6$. Therefore, the base kinetic energy is only 4% (on average) larger than that of the unoscillated flow whereas the best increase in the energy threshold we have found is approximately 41%.

4. Discussion

At the heart of our calculations reported here is a nonlinear optimisation problem with the Navier-Stokes equations as a constraint and the important assumption that the global optimal - the disturbance of a given initial norm which achieves the largest energy gain at the end of a given period - has been identified, using a relatively new variational iterative method which has been recently applied to several canonical flows (see also Pringle & Kerswell (2010); Cherubini *et al.* (2010, 2011); Monokrousos *et al.* (2011); Pringle *et al.* (2012); Rabin *et al.* (2012); Duguet *et al.* (2013); Cherubini & De Palma (2013)). Since this problem is nonlinear and non-convex, proof of global optimality is not ever likely to materialise. However, one can still gather supporting evidence for this

claim by considering a suite of different starting guesses in the optimisation algorithm and recovering the same optimal (e.g. see figures 14 and 15 of Pringle *et al.* (2012)). As further reassurance, recently two groups have found what looks to be the *same* minimal seed in PCF using variational problems built around *different* functionals (total dissipation in Monokrousos *et al.* (2011) and energy gain at the end of a given period in Rabin *et al.* (2012)).

In terms of effort, there is no escaping the fact that the method is computationally expensive. Typically, $O(50)$ iterations are needed in our calculations (each requires integrating the Navier-Stokes equations forwards and 'backwards' across $[0, T]$) to identify the optimal solution at a given set of parameters (here Re, ω, A and ϕ). Given enough cpu flops, there is no reason why the method cannot be scaled up to much larger (realistic) domains, with the detailed dependence of the ensuing drag reduction on amplitude, frequency and flow Reynolds number being determined. Realistically, however, this fully nonlinear approach is not currently competitive with other approximate methods for real-time decision-making in a feedback control context. Such approximate methods can generate sub-optimal but nevertheless useful answers much more quickly. For example, Jovanović (2008) conducted a sensitivity analysis of the linearised Navier-Stokes equations in laminar PCF subject to spanwise oscillations of a single wall and found an 'optimal' oscillation frequency of $5/Re$ which is only just under a half of that found here. But computers are only getting more powerful and it is not hard to imagine that nonlinear strategies will eventually come to the fore.

In summary, we have demonstrated, by using a nonlinear variational method, that it is possible to stabilize PCF in an energetically efficient manner by imposing spanwise oscillations. There is a 'sweet spot' in the amplitude and frequency of the spanwise oscillations where the spanwise shear is sufficiently strong and reaches far enough from the walls to stabilize disturbances which would otherwise trigger transition. The key new capability demonstrated here is that we are able to *quantify* how the disturbance threshold to trigger transition has moved under boundary manipulation, and to *identify* the structure of the new 'minimal seed', i.e. the most dangerous initial perturbation. It should be clear that this method is a very valuable new tool in analysing the nonlinear behaviour of, for example, wall-bounded shear flows where classical linear analysis around the basic state is known to be irrelevant.

Acknowledgements

SMER would like to thank J. R. Taylor for his assistance with the installation and use of the Diablo CFD solver, S. B. Dalziel and A. Holyoake for their invaluable help with other computational issues, G. Chandler for insightful discusions, and the constructive and valuable comments of three anonymous referees which have led to a substantially improved discussion. SMER is supported by a doctoral training award from EPSRC. This work was performed using the Darwin Supercomputer of the University of Cambridge High Performance Computing Service (http://www.hpc.cam.ac.uk/), provided by Dell Inc. using Strategic Research Infrastructure Funding from the Higher Education Funding Council for England. The research activity of CPC is supported by EPSRC Research Grant EP/H050310/1 'AIM (Advanced Instability Methods) for Industry'.

REFERENCES

Baron, A. & Quadrio, M. 1996 Turbulent drag reduction by spanwise wall oscillations. *Appl. Sci. Res.* **55**, 311–326.

Bewley, T. R. 2001 Flow control: new challenges for a new renaissance. *Prog. Aerosp. Sci.* **37**, 21–58.

Bottin, S. & Chate, H. 1998 Statistical analysis of the transition to turbulence in plane Couette flow. *Eur. Phys. J. B* **6** (1), 143–155.

Cherubini, S. & De Palma, P. 2013 Nonlinear optimal perturbations in a Couette flow: bursting and transition. *J. Fluid Mech.* **716**, 251–279.

Cherubini, S., De Palma, P., Robinet, J. C. & Bottaro, A. 2010 Rapid path to transition via nonlinear localized optimal perturbations in a boundary-layer flow. *Phys. Rev. E* **82**, 066302.

Cherubini, S., De Palma, P., Robinet, J.-C. & Bottaro, A. 2011 The minimal seed of turbulent transition in the boundary layer. *J. Fluid Mech.* **689**, 221–253.

Duguet, Y., Monokrousos, A., Brandt, L. & Henningson, D. S. 2013 Minimal transition thresholds in plane Couette flow. *Phys. Fluids* **25** (8), 084103.

Duque-Daza, C., Baig, M. F., Lockerby, D. A., Chernyshenko, S. & Davies, C. 2012 Modelling turbulent skin-friction control using linearized Navier-Stokes equations. *J. Fluid Mech.* **702**, 403–414.

Högberg, M., Bewley, T. R. & Henningson, D. S. 2003 Linear feedback control and estimation of transition in plane channel flow. *J. Fluid Mech.* **481**, 149–175.

Jovanović, M. R. 2008 Turbulence suppression in channel flows by small amplitude transverse wall oscillations. *Phys. Fluids* **20**, 014101.

Jung, W. J., Mangiavacchi, N. & Akhavan, R. 1992 Suppression of turbulence in wall-bounded flows by high frequency spanwise oscillations. *Phys. Fluids A* **4**, 1605.

Juniper, M. P. 2011 Triggering in the horizontal Rijke tube: non-normality, transient growth and bypass transition. *J. Fluid Mech.* **667**, 272–308.

Kasagi, N., Suzuki, Y. & Fukagata, K. 2009 Systems-based feedback control of turbulence for skin friction reduction. *Ann. Rev. Fluid Mech.* **41**, 231–251.

Kawahara, G. 2005 Laminarization of minimal plane couette flow: Going beyond the basin of attraction of turbulence. *Phys. Fluids* **17**, 041702.

Kim, J. & Bewley, T. R. 2007 A linear systems approach to flow control. *Ann. Rev. Fluid Mech.* **39**, 383–417.

Laadhari, F., Skandaji, L. & Morel, R. 1994 Turbulence reduction in a boundary layer by local spanwise oscillating surface. *Phys. Fluids* **6**, 3218–3220.

Lieu, B. K., Moarref, R. & Jovanović, M. R. 2010 Controlling the onset of turbulence by streamwise travelling waves. part 2. direct numerical simulation. *J. Fluid Mech.* **663**, 100–119.

Manneville, P. 2008 Understanding the sub-critical transition to turbulence in wall flows. *Pramana* **70**, 1009–1021.

Moarref, R. & Jovanović, M. R. 2010 Controlling the onset of turbulence by streamwise travelling waves. part 1. receptivity analysis. *J. Fluid Mech.* **663**, 70–99.

Moarref, R. & Jovanović, M. R. 2012 Model-based design of transverse wall oscillations for turbulent drag reduction. *J. Fluid Mech.* **707**, 205–240.

Monokrousos, A., Bottaro, A., Brandt, L., DiVita, A. & Henningson, D. S. 2011 Nonequilibrium thermodynamics and the optimal path to turbulence in shear flows. *Phys. Rev. Lett.* **106** (13), 134502.

Mullin, T. & Kerswell, R. R. 2005 *IUTAM Symposium on Laminar-Turbulence Transition and Finite Amplitude Solutions*. Springer.

Peixinho, J. & Mullin, T. 2007 Finite-amplitude thresholds for transition in pipe flow. *J. Fluid Mech.* **582**, 169–178.

Pringle, C. C. T. & Kerswell, R. R. 2010 Using nonlinear transient growth to construct the minimal seed for shear flow turbulence. *Phys. Rev. Lett.* **105** (15), 154502.

Pringle, C. C. T., Willis, A. P. & Kerswell, R. R. 2012 Minimal seeds for shear flow turbulence: Using nonlinear transient growth to touch the edge of chaos. *J. Fluid Mech.* **702**, 415–443.

Quadrio, M. 2011 Drag reduction in turbulent boundary layers by in-plane wall motion. *Phil. Trans. R. Soc. A* **369**, 1428–1442.

Rabin, S. M. E., Caulfield, C. P. & Kerswell, R. R. 2012 Triggering turbulence efficiently in plane Couette flow. *J. Fluid Mech.* **712**, 244–272.

Romanov, V. A. 1973 Stability of plane-parallel Couette flow. *Functional Anal. Applics.* **7**, 137–146.

Schmid, P. J. 2007 Nonmodal stability theory. *Ann. Rev. Fluid Mech.* **39**, 129–162.

Schmid, P. J. & Henningson, D. S. 2001 *Stability and Transition in Shear Flows*. Springer.

Taylor, J. R. 2008 Numerical Simulations of the Stratified Oceanic Bottom Boundary Layer. PhD thesis, University of California, San Diego.